OPTOELECTRONICS AND ADVANCED MATERIALS – RAPID COMMUNICATIONS Vol. 13, No. 7-8, July-August 2019, p. 487-491

Photocatalytic degradation of organic pollutants using glass fibers supported CdZnS/TiO_2 composite

W. CHANG[a,*], X. Z. HUANG[a], M. J. ZHANG[a], Y. P. DU[a], Y. X. YANG[b]
[a]*College of Environmental and Chemical Engineering, Xi'an Polytechnic University, Xi'an 710048, P. R. China*
[b]*College of Natural, Applied and Health Sciences, Kean University, 1000 Morris Avenue, Union, New Jersey 07083, USA*

The CdZnS/TiO_2 was successfully loaded on the glass fibers by sol-gel process and hydrothermal method. The samples were characterized by scanning electron microscopy, X-ray diffraction, Fourier transform infrared spectrometry and BET analysis etc. The degradation efficiency of CdZnS/TiO_2/GF to methylene blue (MB) reached to 97%. The photocatalytic activity can be ascribed to the beneficial microstructure and synergistic effects of coupled CdZnS/TiO_2 on glass fibers. Therefore, the glass fibers were proved to be a good support for preparation of CdZnS/TiO_2/GF composite which not only exhibited high photocatalytic activity but also was easy to be recycled and reused.

(Received October 14, 2018; accepted August 20, 2019)

Keywords: Photocatalysis, Glass fiber, CdZnS/TiO_2, Sol-gel process

1. Introduction

The development of the society not only brings the progress of mankind, but also brings the serious environmental pollution problems, especially, the water pollution. A safe, effective and inexpensive method to purify water is very important and imperative [1,2,3]. Solar light as a sustainable energy resource is clean, unlimited and globally available. By using solar light, photocatalytic degradation of organic pollutants is an eco-friendly approach to treat environmental contamination [4, 5, 6].

Titanium dioxide (TiO_2), as one of the most popular photocatalysts, has been extensively studied because of its high catalytic reactivity, nontoxic, chemical stability, and low cost. However, a great limitation of TiO_2 is derived from its low utilization rate of solar light. Only can it utilize 2-3% of solar light [7, 8]. Therefore, in the field of photocatalyst study, extending the utilization range of solar energy has become the hot topics in recent years. The methods of doping the transition metals additives[9,10,11], rare earth metals[12,13,14], non-metals[15,16,17,18,19], combined with other semiconductors[20,21,22,23], sensitizers etc.[24,25]on TiO_2 have been studied for expanding the light response range of TiO_2. As a kind of p type semiconductor with narrow band gap of 2.42 eV, CdS coupled with TiO_2 proved to improve the optical absorption properties and photocatalytic activity effectively [26, 27]. When Zn was introduced to CdS to develop the CdZnS solid solutions, the stability and photoactivity of the material was further improved according to the report [28, 29]. The introduction of Zn can act as the band participants rather than recombination centers [30]. Therefore, it is expected that coupling TiO_2 with the CdZnS solid solutions may exhibit enhanced efficient and stable photocatalytic performance [31,32,33]. However, most of TiO_2 with the CdZnS were produced in powder form, which have become the thorny problem to be overcome when they were used in treating wastewater. Thus some studies have focused on loading powder photocatalysts onto suitable supports. An assortment of materials, such as silica, zeolites, activated carbon and glass fiber has been used to immobilize nanoparticles [34,35,36]. Among them, the glass fiber with high temperature resistance, acid and alkali resistance, corrosion resistance, high mechanical strength, light transmission, and chemical stability, is widely used as a support in various applications [37,38,39]. The glass fiber can make the catalyst evenly distributed, increase the contact area between the catalyst and the wastewater, and promote photocatalytic efficiency.

In this study, the glass fiber was chosen as the support to composite of TiO_2 and CdZnS by sol-gel process and hydrothermal method. The photocatalytic activity and reuse feasibility of the glass fibers supported CdZnS/TiO_2 composite was evaluated by degradation of MB under 500W xenon lamp irradiation.

2. Experimental

2.1. Materials

Methanol (CH_3OH), polyethylene glycol (PEG, $H(OCH_2CH_2)_nOH$, 10000), acetic acid (CH_3COOH, 99%), urea (CH_4N_2O), butyl titanate ($Ti(OC_4H_9\text{-}n)_4$), zinc acetate ($(CH_3COO)_2Zn\cdot 2H_2O$), cadmium acetate ($(CH_3COO)_2Cd\cdot 2H_2O$), thiourea (CN_2H_4S), sodium hydroxide (NaOH) were obtained of analytical purity grade and were directly used without further purification. Glass fibers (GF) were provided by Shaanxi Hua Tek Fiberglass Material Group Co. Ltd.

2.2. Preparation of samples

Firstly, the glass fibers were pre-treated with HCl at 80℃ for 1h, washed by deionized water and dried in an oven. The TiO_2/GF was prepared by sol-gel process. Typically, 0.6 g urea, 0.64 g polyethylene glycol and 4 mL butyl titanate were sequentially added to the solution containing 12 mL methanol and 2 mL acetic acid. The mixture was continuously stirred for 30 min to form the sol. Then pre-treated glass fibers were immersed in the sol for 1 min followed by keeping the fibers in an oven at 40℃ for 10 hrs and calcined at 500℃ for 6 hrs.

CdZnS/GF was prepared by hydrothermal method. 2 mmol zinc acetate, 2 mmol cadmium acetate and 5 mmol thiourea were dissolved in 26 mL of deionized water, the mixture was continuously stirred for 1 h. The obtained solution and pre-treated glass fibers were transferred into a sealed reactor and heated at 160℃ for 8 h. And then, the glass fiber composites were washed by deionized water for 5 times and dried at 80℃ overnight.

CdZnS/TiO_2/GF was prepared by combining the sol-gel process and hydrothermal method. According to the preparation process of CdZnS/GF, the pre-treated glass fibers were replaced by TiO_2/GF to prepare the CdZnS/TiO_2/GF.

2.3. Characterization

The morphology of all the samples were observed by scanning electron microscopy (SEM) performed on a QUATA FEG 450 field emission instrument operated at an accelerating voltage of 5.0 kV. The crystal structure of the samples were analyzed by XRD (Rigaku，Dmax-Rapid II) with CuKα radiation (λ=0.15418 nm, 40 kV, 40 mA). The scanning range was from 20° to 90°. The infrared absorption spectroscopy was measured with a Perkin Elmer Frontier spectrophotometer. The surface areas of samples were determined using a 2390 Micromertics instrument. UV-vis diffuse reflectance spectra were recorded at room temperature on a Lambda 950.

2.4. Photocatalytic efficiency

Photocatalytic performance of the prepared samples was investigated by degrading MB simulated wastewater. The photocatalytic experiments were conducted in a photocatalytic reactor (XPA). In the experiment, a 500W xenon lamp was used as the light source, prior to irradiation, 30 mL of MB (2×10^{-5} mol/L)aqueous solutions containing 30 mg sample were magnetically stirred in the dark for 60 min to achieve adsorption/desorption equilibrium and a good dispersion. During the photoreaction, the samples were collected at regular intervals (20 min) and centrifuged to remove the sample. The supernatant solution was analyzed by an UV-visible spectrophotometer (UV-2450, Shimadzu) at 664 nm.

3. Results and discussion

3.1. SEM of the As-prepared materials

Fig. 1 shows the SEM images of the prepared samples. It can be observed that the surface of GF is smooth (Fig. 1 (a)). Fig. 1 (b) shows that the glass fiber was enclosed by a TiO_2 layer in fragments. CdZnS/GF in Fig. 1 (c) can be observed that CdZnS particles load on the GF by hydrothermal method and have a relatively uniform distribution. By the hydrothermal process, the morphology of TiO_2 has an obvious change. The TiO_2 fragments were changed to continuous flakes, and CdZnS were embedded in them to form CdZnS/TiO_2 heterostructure coating on the glass fibers, which can be observed in Fig. 1 (d).

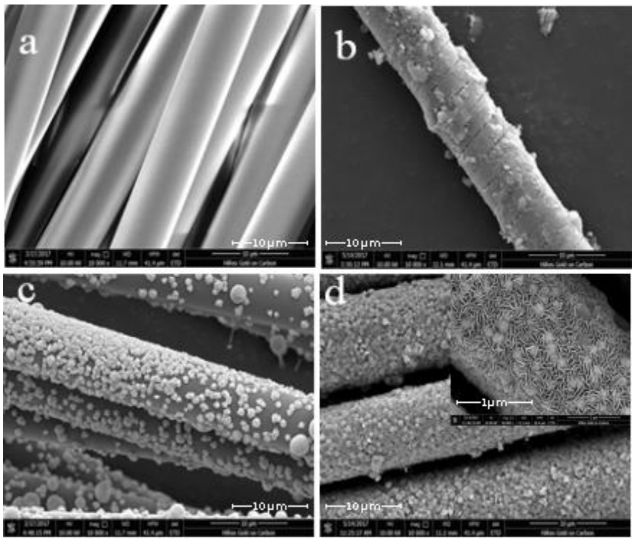

Fig. 1. SEM images of (a) GF (b) TiO_2/GF (c) CdZnS/GF and (d) CdZnS/TiO_2/GF.

3.2. X-Ray Diffraction (XRD) Patterns

The XRD patterns of GF, TiO_2/GF, CdZnS/GF and CdZnS/TiO_2/GF samples are shown in Fig. 2. It can be observed that the diffraction peak of GF appear a taro-like peak at about 20°, indicating that GF exist in amorphous phase. TiO_2/GF pattern consists of two sets of diffraction peaks, which belong to anatase TiO_2 and rutile TiO_2, respectively. The peaks appearing at 37.0° (200), 43.0° (402), 47.1° (133), 52.9° (201), 61.3° (214), 68.7° (103), and 73.7° (220), which are consistent with the anatase TiO_2 (JCPDS No. 21-1272). The characteristic peak appearing at 24.9° (110) coincides with the rutile TiO_2 (JCPDS No. 65-0190). The results show that the TiO_2 in TiO_2/GF is an anatase-based mixed crystal. The diffraction peaks of CdZnS/GF appear at 24.8° (100), 25.8° (130), 27.8° (040), 43.2° (101), 47.1° (220), and 51.3° (771), which are consistent with the hexagonal crystal CdZnS

(JCPDS No.40-0836). It can be seen that the diffraction peaks of CdZnS/TiO_2/GF include anatase TiO_2 (47.9°), rutile TiO_2 (24.9°) and hexagonal crystal CdZnS(26.5°, 28.2°, 43.8°, 51.9°). Therefore, TiO_2 and CdZnS are loaded on the GF successfully.

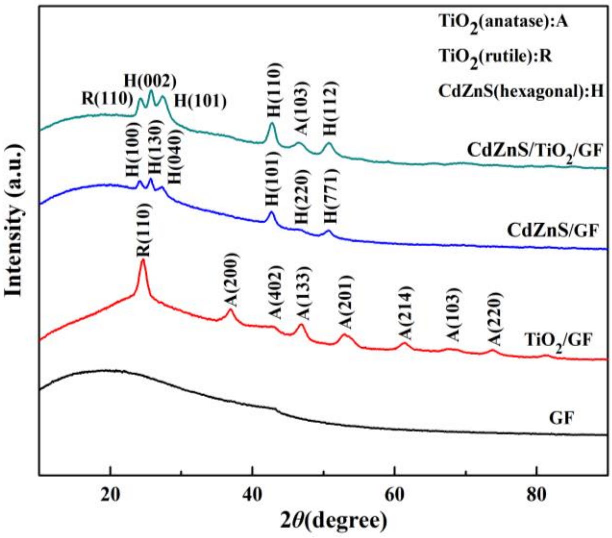

Fig. 2. XRD patterns of the prepared samples

3.3. FTIR Spectra

FTIR spectra of the prepared samples are shown in Fig. 3. For the TiO_2/GF, the peak at 1040 cm^{-1} corresponds to the Si-O-Si stretching vibration; the characteristic peaks at 893 cm^{-1} can be assigned to the Si-O-Ti stretching vibration. For the CdZnS/GF, the peak at 1007 cm^{-1} belongs to the Si-O-Si stretching vibration; and the peak at 788cm^{-1} comes from the Cd-S or Zn-S bond. For the CdZnS/TiO_2/GF, the peak at 1020 cm^{-1} corresponds to the Si-O-Si stretching vibration; the peaks at 893 and 774 cm^{-1} belongs to the Si-O-Ti stretching vibration and the Cd-S or Zn-S bond.

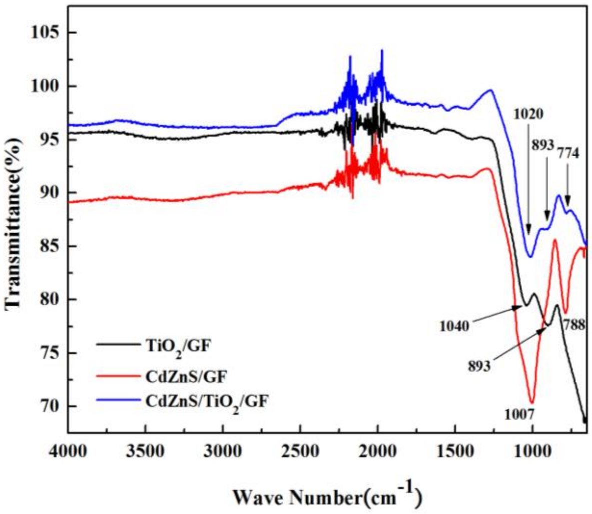

Fig. 3. FTIR spectra of the prepared samples

3.4. Nitrogen adsorption-desorption

The nitrogen adsorption-desorption isotherms and the pore size distribution curves of the prepared samples are shown in Fig. 4 and its inside. For the TiO_2/GF, the nitrogen adsorption-desorption isotherms shows a typical type IV pattern with nitrogen adsorbed volume at P/P_0 about 0.46 (type H1 hysteretic loop), indicating the mesoporous structure of the sample. The pore size distribution curve of the sample (inset in Fig. 4) indicates that the TiO_2/GF exhibits the largest pore volume of 0.59cm^3/g and the pore size of 6.9 nm. The specific surface area is 130.5m^2/g. For the CdZnS/TiO_2/GF, the isotherms exhibits type IV isotherm with a type H1 hysteretic loop at P/P_0 about 0.66. The pore size distribution curve of the sample (inset in Fig. 4) indicates that the CdZnS/TiO_2/GF exhibits the largest pore volume of 0.08cm^3/g and the pore size of 6.9 nm. The specific surface area is 18.63m^2/g. While for the CdZnS/TiO_2/GF, the pore volume and the specific surface area are significantly decreased, and the peak center is shifted to 3 nm which could be attributed to the piled pore of secondary particles. The results suggest that CdZnS loading would affect the porous structure of the TiO_2.

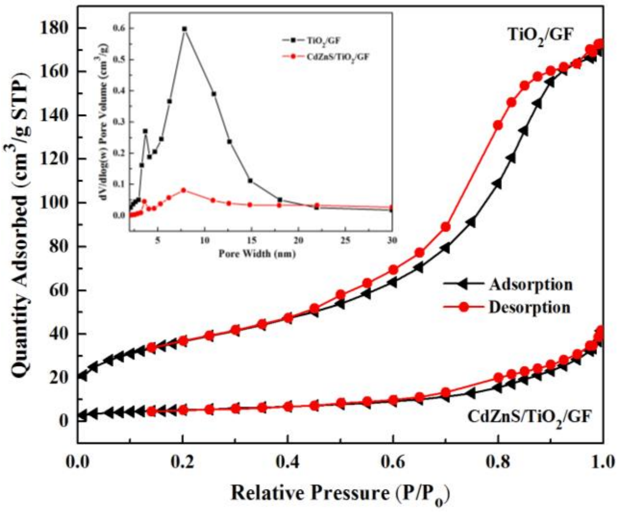

Fig. 4. Nitrogen adsorption-desorption isotherms and pore size distribution curves of the prepared samples

3.5. UV-vis DRS spectrum

Fig. 5 shows the UV-vis DRS spectrum of the prepared samples. It can be observed that TiO_2/GF absorbs only in the ultraviolet region, while the absorption of CdZnS/GF and CdZnS/TiO_2/GF extends to the visible region. According to the extension method [8], the light absorption threshold and forbidden band gap of the prepared samples were evaluated and the results are shown in Table 1.

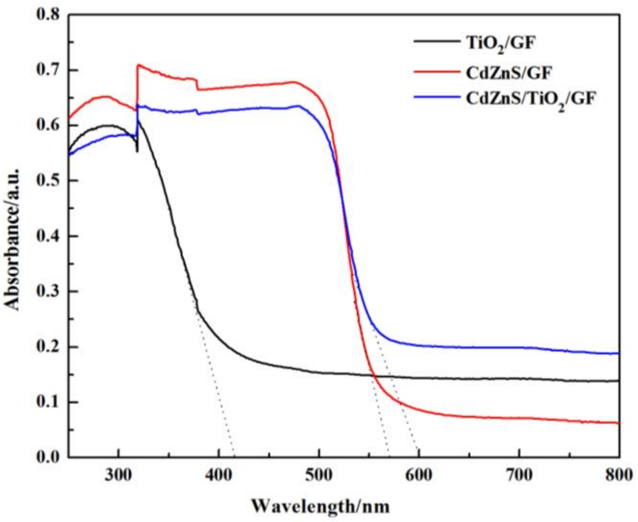

Fig. 5. UV-vis DRS spectrum of the prepared samples

Table 1. Light absorption threshold and forbidden band width of the prepared samples

sample	TiO_2/GF	CdZnS/GF	$CdZnS/TiO_2/GF$
λg(nm)	429	598	616
Eg(eV)	2.89	2.07	2.01

The band gap of TiO_2/GF was calculated to be 2.89 eV, while those for CdZnS/GF and $CdZnS/TiO_2/GF$ were valuated to be 2.07 eV and 2.01 eV, respectively. These values demonstrate that CdZnS/GF and $CdZnS/TiO_2/GF$ exhibit strong absorption in both visible light and UV regions.

3.6. Photocatalytic activity

The photocatalytic activities of the glass fiber composites were evaluated by degradation of MB dye in water (Fig. 6). The original concentration of MB solution is 2×10^{-5} mol/L. It can be seen in Fig. 6, after 60 min of adsorption equilibrium, the adsorption amount of MB on $CdZnS/TiO_2/GF$ is the greatest in comparison with the others. Under 500 W xenon lamp irradiation, the $CdZnS/TiO_2/GF$ possess enhanced photocatalytic efficiency in photodegradation of MB (degradation efficiency reaches 97%) and exhibit the highest degradation efficiency among the prepared samples. The enhanced photocatalytic activity of $CdZnS/TiO_2/GF$ is attributed to its structure. $CdZnS/TiO_2/GF$ have the narrowest band gap, which can make full use of visible light and allow more excited electrons to migrate to the conduction band, increase the number of carriers and then promote the photocatalytic degradation reaction.

Considering the practical application, it is important that the photocatalyst maintains high activity and stability for a long-term use. Therefore, the recycling experiments were conducted to test the reusability of the $CdZnS/TiO_2/GF$, and all experiments were carried out under the same conditions.

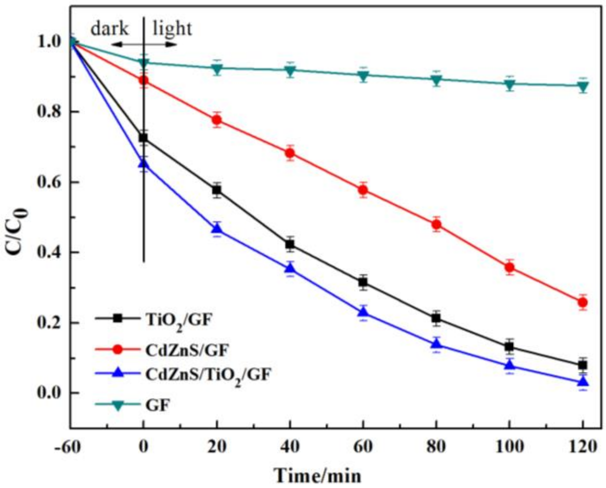

Fig. 6. Photocatalytic activity of the prepared samples

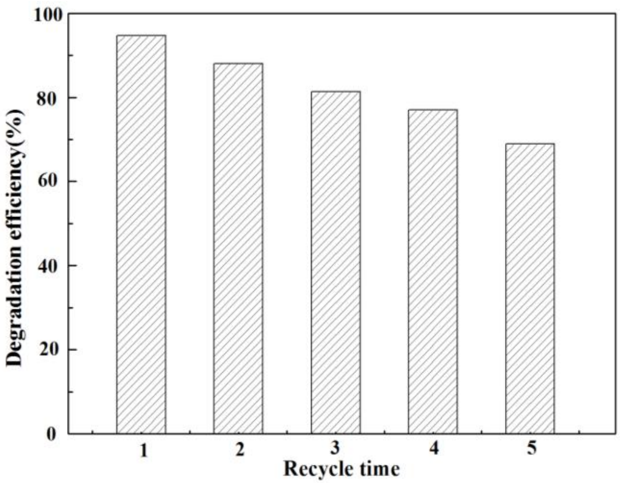

Fig. 7. Photocatalytic activity of the $CdZnS/TiO_2/GF$ for MB degradation with five-times recycle uses

As shown in Fig. 7, the $CdZnS/TiO_2/GF$ still has high photocatalytic activity after five times repeated use. The result shows that the $CdZnS/TiO_2/GF$ has great potential in the removal of organic pollutants.

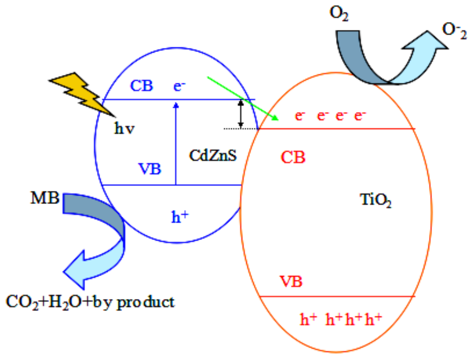

Fig. 8. Schematic illustration of photocatalytic mechanism [8].

Schematic illustration of photocatalytic mechanism of the CdZnS/TiO$_2$ heterostructure is shown in Fig. 8. In this structure, CdZnS with relatively narrow band gap serves as sensitizer, since it can be excited by visible light. Upon visible light irradiation, electrons in the VB of CdZnS are excited to the CB with higher potential edge, while holes are left on the VB. The photogenerated electrons can transfer easily from CB of CdZnS to that of substrate TiO$_2$ owing to band alignment and potential difference. On the other hand, the heterojunction between CdZnS and TiO$_2$ are helpful for photogenerated electrons transfer and further prevent the recombination between photogenerated charge carries. The photoinduced electrons accumulated on the CB of TiO$_2$ are scavenged immediately by oxygen adsorbed on the surface of TiO$_2$ or dissolved in the water to yield the superoxide radical anion O_2^-, which could combine with H^+ to form $HO_2\cdot$ and H_2O_2. This newly formed intermediate products can interact to form the hydroxyl radical (HO·), which is considered as a strong oxidizing agent to degrade MB. Meanwhile, the holes stay in the VB of CdZnS layer can degrade MB directly.

4. Conclusions

In summary, the CdZnS/TiO$_2$/GF was prepared by sol-gel process and hydrothermal method. The CdZnS/TiO$_2$ were successfully loaded on the GF surface and show enhanced photocatalytic activity in degradation of MB when 500 W xenon lamp irradiation. The cycling experiments indicated that the CdZnS/TiO$_2$/GF has better reusability and is easy to be recycled. It may be considered a promising material for practical application in wastewater treatment.

Acknowledgements

This work is supported by the Science and Technology Department Research Funds of Shannxi Province, China (2018GY-131) and Research and Development Program of Beilin District, Xi'an, China (GX1808) and National Natural Science Foundation of China (21703165).

References

[1] A. Y. Zhang, W. K. Wang, D. N. Pei, Water Res. **92**, 78 (2016).
[2] L. Wang, M. Wen, W. Wang, J. Alloy. Compd. **83**, 318 (2016).
[3] R. G. Nair, S. Mazumdar, B. Modak, A: Chem. **345**, 36 (2017).
[4] A. Khan, R. Khan, A. Waseem, Inorg. Chem. Commun.**72**, 33 (2016).
[5] S. Sood, A. Umar, S. K. Mehta, J. Colloid Interf. Sci. **450**, 213 (2015).
[6] D. Tomova, V. Iliev, A. Eliyas, Sep. Purif. Technol. **156**, 715 (2015).
[7] X. Li, D. Yin, S. Kang, J. Mu, J. Wang, G. Li, Colloids Surf. A: Physicochem. Eng. Asp. **384**, 749 (2011).
[8] G. Yang, Q. Zhang, W. Chang, W. Yan, J. Alloy. Compd. **580**, 29 (2013).
[9] L. Qin, X. Pan, L. Wang, Appl. Catal. B: Environ. **150**, 544 (2014).
[10] Y. Deng, M. Xing, J. Zhang. Appl. Catal. B: Environ. **211**,157 (2017).
[11] B. Kılıç, N. Gedik, S. P. Mucur, Mat. Sci. Semicon. Proc. **31**, 363 (2015).
[12] M. Khan, W. Cao, Mater. Res. Bull. **49**, 21 (2014).
[13] Z. Hao, M. Song, F. Yi, L. Bian, P. Liu, S. Zhang, J. Alloy. Compd. **680**, 54 (2016).
[14] D. Liu, Z. Wu, F. Tian, B. Ye, Y. Tong, J. Alloy. Compd. **676**, 489 (2016).
[15] S. Xu, X. Sun, Y. Zhao, Y. Gao, Y. Wang, Appl. Surf. Sci. **448**, 78 (2018).
[16] S. Ramandi, M. H. Entezari, N. Ghows, Ultrason. Sonochem. **38**, 234 (2017).
[17] F. Li, J. Zhou, C. Du, J. Environ. Sci. **60**, 24 (2017).
[18] Y. Zou, J. W. Shi, D. Ma, Chem. Eng. J. **322**, 435 (2017).
[19] R. A. Senthil, J. Theerthagiri, A. Selvi, Opt. Mater. **64**, 533 (2017).
[20] V. Šteng, D. Králová, Int. J. Photoenergy **2011**, 16638 (2011).
[21] V. Daskalaki, M. Antoniadou, G. Puma, D. Kondarides, P. Lianos, Environ. Sci. Technol. **44**, 7200 (2010).
[22] X. Li, D. Yin, S. Kang, J. Mu, J. Wang, G. Li, Colloids Surf. A: Physicochem. **384**, 749 (2011).
[23] Y. F. Chai, G. F. Huang, L. L. Wang, W. Q. Huang, J. Zhou, Mater. Lett. **142**, 133 (2015).
[24] B. Tian, R. Dong, J. Zhang, Appl. Catal. B: Environ. **158**, 76 (2014).
[25] B. Wang, H. Zhang, X. Y. Lu, Chem. Eng. J. **253**, 174 (2014).
[26] Y. Zhu, R. Wang, W. Zhang, Appl. Surf. Sci. **315**, 149 (2014).
[27] B. Pant, N. A. M. Barakat, H. R. Pant, J. Colloid. Interf. Sci. **434**, 159 (2014).
[28] A. Hospodková, L. Svoboda, P. Praus, Chinese J. Catal. **36**, 328 (2015).
[29] C. V. Reddy, J. Shim, M. Cho, Synthesis, J. Phys. Chem. Solids **103**, 209 (2017).
[30] P. Praus, L. Svoboda, J. Tokarský, Appl. Surf. Sci. **292**, 813 (2014).
[31] M. Antoniadou, V. M. Daskalaki, N. Balis, Appl. Catal. B-Environ. **107**, 188 (2011).
[32] L. Zhu, Z. D. Meng, C. Y. Park, Ultrason. Sonochem. **20**, 478 (2013).
[33] A. Arabzadeh, A. Salimi, J. Colloid. Interf. Sci. **479**, 43 (2016).
[34] W. J. Zhang, Y. J. Tao, C. G. Li, M. R. Bull. **105**, 55 (2018).
[35] W. J. Zhang, Y. J. Tao, C. G. Li, J. Photochem. Photobio. A: Chem. **364**, 787 (2018).
[36] W. J. Zhang, F. F. Bi, Y. Yu, H. B. He, J. Mol. Catal. A-Chem. **372**, 6 (2013).
[37] H. Meng, W. Hou, X. Xu, Particuology **14**, 38 (2014).
[38] R. K. Nayak, K. K. Mahato, B. C. Ray. Compos. Part A: Appl. Sci. Manufac. **90**, 736 (2016).
[39] T. D. Pham, B. K. Lee, Appl. Surf. Sci. **296**, 15 (2014).

---

[*] Corresponding author: changwei72@163.com